17th World Conference on Earthquake Engineering, 17WCEE
Sendai, Japan - September 13th to 18th 2020

Influence of flange local buckling of I-shaped braces on the seismic response of concentrically steel braced frames

B. Hariri[(1)], R. Tremblay[(2)]

[(1)] PhD Candidate, Dept. of Civil, Geological and Mining Engineering, Polytechnique Montréal, bashar.hariri@polymtl.ca
[(2)] Professor, Dept. of Civil, Geological and Mining Engineering, Polytechnique Montréal, robert.tremblay@polymtl.ca
…

Abstract

This paper proposes a technique to account for the local buckling of flanges when modelling concentric I-shape bracing members in OpenSees. The proposed modelling approach makes use of the fiber removal technique where fibers near the edge of the flanges are removed to reduce the sectional capacity in both compression and flexure and, thereby, simulate the strength reduction due to local buckling. Fatigue material with optimizable failure parameters was used as a trigger to remove the flange fibers. The number of fibers allowed to reach fatigue as well as the fatigue parameters are adjusted through an optimization process to match the results of cyclic tests on braces. Thus, the optimization is carried out at the element and material levels, instead of material-only level. In the first part of the article, the model is calibrated against the results of quasi-static cyclic tests performed on full-scale brace specimens at Polytechnique Montréal. The proposed modelling technique improved the prediction of the load-deformation response in the post-buckling range as well as the yielding plateau upon reloading in tension. The second part of the article evaluates the effects of brace local buckling on the structural response of 2- and 4-storey frames using nonlinear time history analysis. The frames were modelled in OpenSees, firstly by using the classical modelling approach for I-braces and, secondly, by using the proposed modelling approach to account for local buckling. It was found that, on average, accounting for local buckling had negligible effects on both peak and residual storey drifts, as these response parameters are mainly controlled by the braces acting in tension.

Keywords: Braced frames; Local buckling; Modelling; OpenSees; Response history analysis.

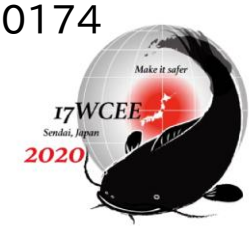

1. Introduction

The concentrically braced frame (CBF) system is very commonly used for resisting lateral loads in steel building structures. Given their simplicity and low cost, CBFs have been used in buildings long before design codes were modified to include special design and detailing provisions to achieve ductile seismic response. Nowadays, modern seismic design provisions [1,2] aim at mitigating the occurrence of local buckling in bracing members by imposing stringent width-to-thickness ratio limits. However, local buckling is a possibility in existing, seismically deficient, steel braced frames and accounting for this behaviour might be necessary for seismic evaluation and rehabilitation purposes. Local buckling of bracing members is also a possibility in braced frames designed for higher seismic loads and that are not detailed for ductile seismic response. Since 1980, several experimental studies have been performed to investigate the inelastic behaviour of steel braces under cyclic loading [3-7]. Tremblay et al. [6] carried out quasi-static cyclic tests on large size, full-scale braces having different shapes and cross-sectional areas, in addition to different global and local slenderness ratios. The study showed that for tubular (HSS) sections, brace fracture occurred soon after initiation of local buckling, typically within the same cycle when the brace was loaded in tension. Conversely, I-shaped braces could withstand several loading cycles after local buckling had developed in their flanges, implying that I-shaped braces can exhibit larger inelastic deformation capacities compared to HSS braces. Similar response was observed by Fell et al. [8], Zeng et al [9] and Shim and Kim [10]. However, their hysteretic response was affected by local buckling as the change in cross-section in the mid plastic hinge reduces the brace compressive strength in the subsequent cycles, which suggests that this behaviour should be considered in the seismic analysis of braced steel frames with I-shaped braces that do not meet special seismic cross-section slender limits. Advanced finite element analysis can be used to properly account for local buckling effects on individual brace response subjected to cyclic loading [11,12]. However, this type of analysis is too computationally extensive to be used for the study of multi-storey steel braced frames subjected to seismic loading.

In the last two decades, the OpenSees finite element analysis software [13] has been extensively used for the seismic analysis of steel braced frames. In this platform, steel bracing members are modelled using nonlinear beam-column elements with fiber discretization of the cross-section [14-17]. In this model, local buckling cannot be reproduced but the technique is well suited for capturing the global buckling response required for nonlinear seismic analysis. Therefore, this model is adequate for new CBFs, given the stringent width-to-thickness ratio limits adapted by modern design codes. However, for the existent deficient braces, this classical modelling might not be appropriate because it cannot reproduce local buckling. Despite these observations, no study has been performed yet to examine the possible impacts of local buckling of I-braces with slender cross-sections on the seismic response of steel braced frames. This article aims at filling this gap in the literature by proposing a simple fiber-removing technique to simulate local buckling of I-section braces modelled with the common nonlinear beam-column element representation in OpenSees. The fatigue model proposed by Zeng et al. [9] is used to reproduce this behaviour, and the properties of the fatigue model are first calibrated using the results of the six quasi-static cyclic tests performed at Polytechnique Montréal [6]. It is important to mention that similar approach was proposed by [18] to account for flange local buckling of I-shaped beams in moment resisting frames (MRFs). The second part of this paper will evaluate the effect of brace local buckling on the nonlinear response of 2- and 4-storey prototype braced frames located in Vancouver, British Columbia, Canada. The mass and geometrical properties of the prototype frames are adjusted such that the braces exactly correspond to the braces tested by Tremblay et al [6] used for the calibration.

2. Brace Modeling

The bracing members are modelled using the nonlinear force-based beam-column elements with fiber discretization of the cross-section that is available in the OpenSees seismic analysis software [12]. Each brace was modelled with a total of 8 elements, each element being assigned 4 integration points using the Gauss-Lobatto numerical integration. The fibers are assigned with the Steel02 material that can account for yielding, Baushinger effect, and kinematic and isotropic hardening responses as expected for steel subjected to cyclic inelastic demand. Out-of-straightness of 1/1000 of the brace length was specified assuming a half-sine wave

initially deformed shape. This model has been successfully used in previous numerical studies to reproduce the inelastic global buckling and yielding responses of steel bracing members subjected to cyclic demand [6, 9, 14, 15, 17].

In the cyclic tests, brace global buckling occurred about the brace weak axis. The same buckling mode was also anticipated in the studied braced frames and the cross-section fiber discretization was adapted to efficiently and accurately simulate the brace response for this condition. To simulate flange local buckling, each flange of the cross-section was discretized into 30x2 fibers in the weak and strong directions, respectively. The web was also discretized into 10x4 fibers in the same directions (Fig. 1a). Giuffré-Menegotto-Pinto material (Steel02) was used with the recommended values for parameters R0 (= 20), CR1 (= 0.925), and CR2 (= 0.15). The stiffness of the splicing plates was considered using an equivalent Young's modulus and the measured yield stress of the test specimens was used. The kinematic hardening parameter b was taken equal to 0.01 and the isotropic parameters were assigned the following values: a1 = 0.001, a2 = 1, a3 = 0, and a4 = 1. Linearly varying initial residual stresses were assigned to the fibers, as proposed by Lamarche and Tremblay [19], with peak compressive stress at the tip of the flanges equal to 0.33 F_y, peak tensile stress at the flange to web intersection equal to 0.66 F_y, and peak compressive stress at the mid-depth of the web as determined to reach equilibrium. To simulate the reduction of sectional capacity due to local buckling, fatigue material with default slope m (= -0.458) was modelled to work in parallel with the Steel02 to form what will be referred to herein as *buckling material*. This material was used on a selected range of flange fibers (Fig. 1a), at the probable location of the plastic hinge (Fig. 1b). Since the fatigue material is used as fiber cancelling tool, and not to simulate the actual fatigue, its strain (ε_0) is a parameter to be calibrated. The range of fiber elements modeled with buckling material (R) is another calibratable parameter, where the number of fibers can vary from zero (no local buckling) to ten covering one third of the flange width. Only the flanges of the middle elements (i.e. elements nos. 4 and 5) were modelled using the above-mentioned *buckling material*, given the region where plastic hinge is expected. To enhance converges, each fiber from the range R was additionally discretized into 30 fibers in the weak direction, as illustrated in Fig. 1a.

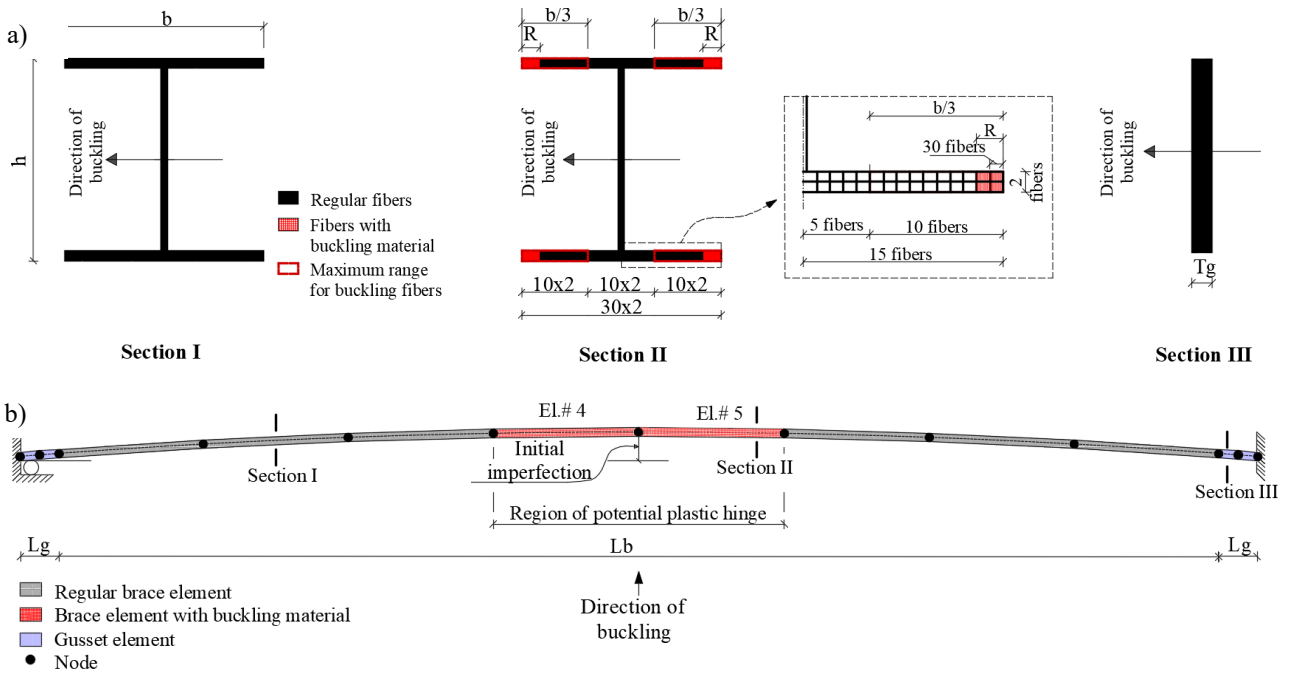

Fig. 1 – Brace modelling description. a) Fiber sections; b) Brace layout

The detail of the brace end connections for one of the test specimens is shown in Fig. 2. As shown, the "$2t_g$" plastic hinge region was located at the end of the splice plates connecting the I-shape brace to the gusset plate. Instead of using nonlinear rotational springs to reproduce the inelastic rotational response of the gusset plate

upon brace buckling, each gusset plate was modelled using two nonlinear beam-column elements with an approximate length (L_g) of twice the gusset plate thickness. The gusset plate section assigned to these elements was discretized using 40 fibers across the gusset plate thickness and 4 fiber across the plate width. Steel02 material was assigned to the fibers, with the same values for as those used for the bracing members, except that no residual stresses were specified.

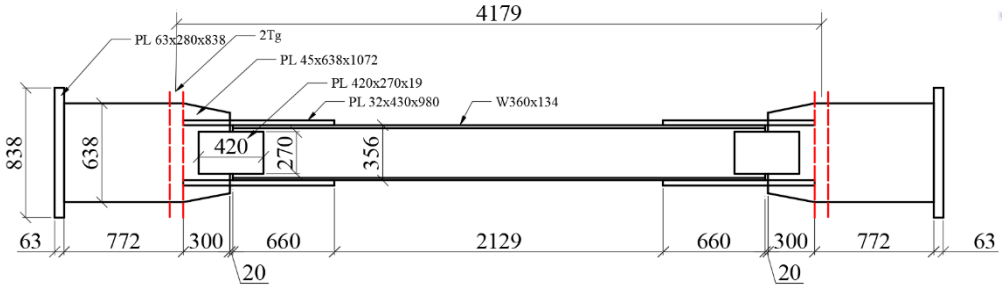

Fig. 2 – Specimen W1 brace-end connections

3. Model calibration

The buckling material parameters (R, ε_0) were calibrated using data of six full-scale specimens tested at Polytechnique Montreal [6]. The specimens varied in area of cross section, global and local slenderness ratios and were tested using quasi-static symmetrical loading protocols. Specifications of the tested specimens are given Table 1. In the tests, flange local buckling was limited to the location of the plastic hinge at the specimen mid-length, and it was mainly governed by the flange width-to-thickness ratio. Only the specimens with low global slenderness ratio and flange width-to-thickness ratio exceeding the CSA-S16 [2] limit ($b/2t \approx 7.8$) developed local buckling. Model calibration was performed using a Matlab routine that minimized the error on the load resisted by the braces between the test and numerical prediction by progressively adjusting the values of the parameters R and ε_0. The so-obtained calibrated values are given in Table 1.

Table 1 – Specification of tested specimens

Specimen number	Section	Length [mm] L_b	Global slenderness KL/r	Flange slenderness $b/2t$	R	ε_0	Number of fibers with *buckling material*
W1	W360x134	4179	40.0	10.25	4	0.060	1920
W2	W310x129	3466	40.0	7.47	3	0.062	1440
W3	W310x129	5200	60.0	7.47	0	–	–
W4	W310x97	5120	60.0	9.90	2	0.060	960
W5	W310x86	4247	60.0	7.79	1	0.056	480
W6	W250x115	4414	59.9	5.85	0	–	–

To evaluate the effect of local buckling on hysteretic behaviour of the I-braces, differences in response when local buckling is neglected-and-considered in the numerical model are presented in Fig. 3a and b, respectively. Only specimens W1, W2, W4, and W5 that developed flange local buckling are presented in the figure (W5 is not presented due to space limitation). As shown, for these three specimens, when compared to the conventional brace models without local buckling, the brace models with the calibrated *buckling material* predict a more severe compressive strength degradation with cycles and reduced brace tensile yielding, consistent with the measured hysteretic responses. These differences were also observed in other past test programs on I-shaped braces in which flange local buckling was observed [6-10, 15]. For specimens W3 and W6 with flanges meeting the CSA S16 width-to-thickness limit, their hysteric behaviour could be well reproduced with numerical models using basic material parameters only, i.e. with the parameter $R = 0$ for the *buckling material*, as presented in Fig. 4.

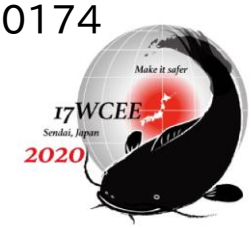

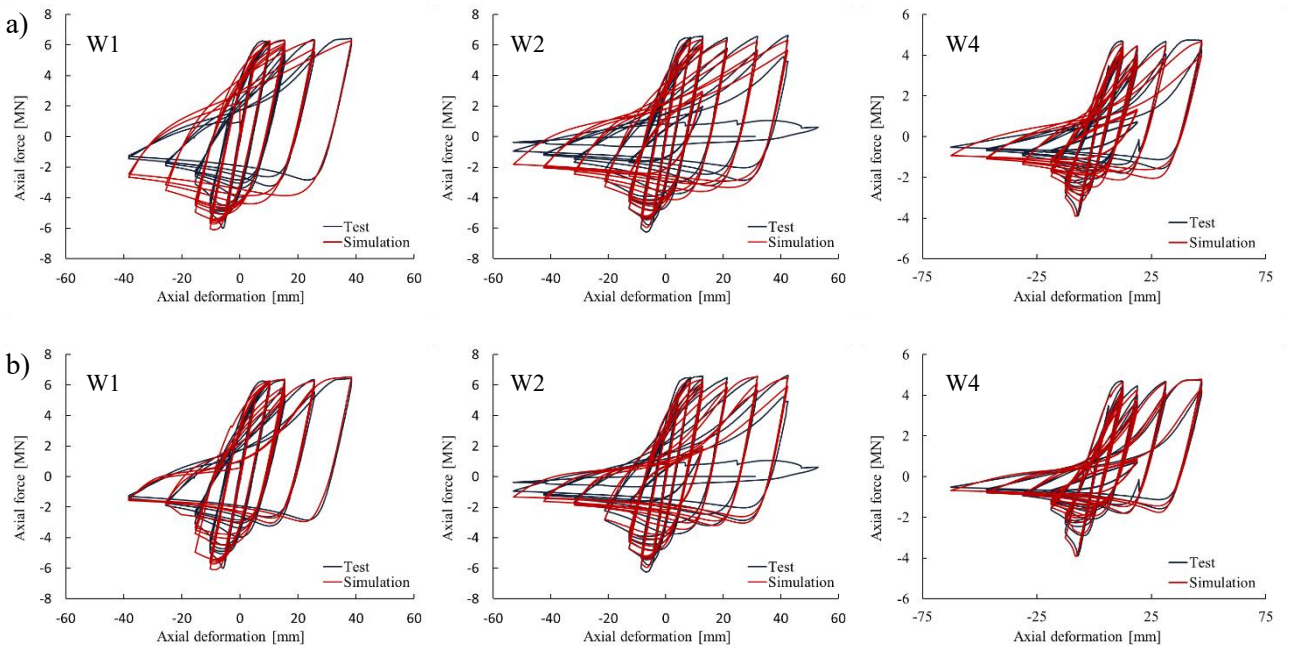

Fig. 3 – Calibration results. a) Without buckling material; b) With buckling material

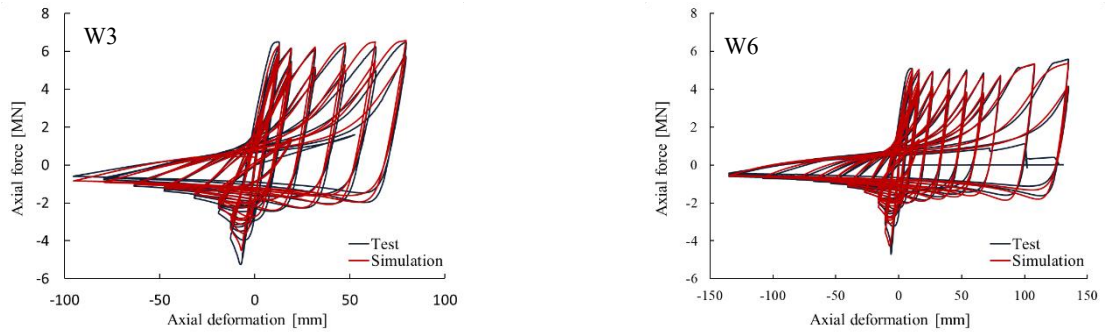

Fig. 4 – Calibration results for specimens W3 and W6

4. Nonlinear analysis of 2- and 4-storey frames

4.1 Frame and ground motion description

Seismic analysis of the 2- and 4-storey prototype frames shown in Fig. 5 was performed to examine the effect of brace local buckling on frame response. The structures were assumed to be located on a class C (firm ground) site in Vancouver, BC, and were designed in accordance with the NBC 2015 building code [1] and the CSA-S16 steel design standard [2]. The braced frames were considered as Type LD (limited ductility) braced frames for which the design seismic loads are obtained using ductility and overstrength related force modification factors equal to 2.0 and 1.3, respectively. All seismic design and detailing provisions were satisfied, except that the width-to-thickness ratio limits for the braces were ignored.

Because the properties of the *building material* for the brace model had been obtained solely from test results, it was decided that the frames would include only braces having the exact same cross-section and length as the brace specimens W1, W2, W4, W5 used in the calibration process. In the frames, braces were selected and positioned to obtain storey shear resistances gradually decreasing from the base to the roof, as would be the case in actual structures, and the storey heights were adjusted to reproduce the brace test lengths. Seismic

weights (and masses) at each level of the frames were then back calculated such that the storey shear demand from response spectrum analysis would match the storey shear resistances provided by the braces. Columns and beams were designed in accordance to capacity design criteria specified in CSA-S16.

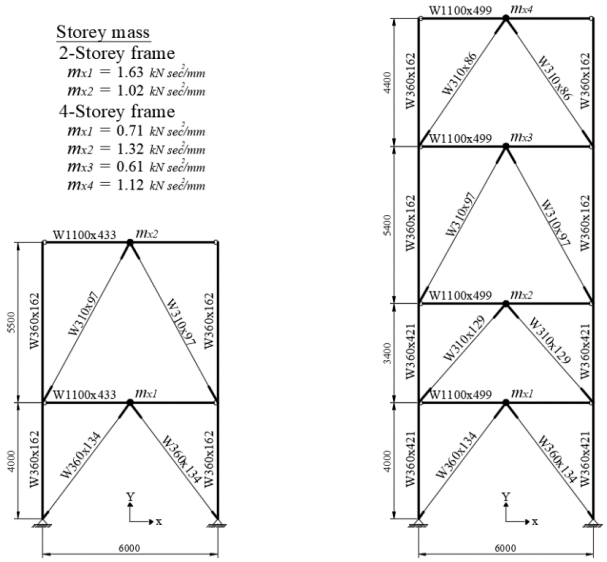

Fig. 5 – Prototype frames

The structures were subjected to an ensemble of 33 ground motion records comprising three suites of 11 ground motions. Each suite contained records representative of the three sources of earthquakes contributing to the seismic hazard in southwest British Columbia, i.e. shallow crustal earthquakes (Suite 1), deep in-slap subduction earthquakes (Suite 2), and interface subduction earthquakes (Suite 3). Selection and scaling of the ground motions was performed in accordance with Method A of the guidelines given in the NBC Commentary [20] (Fig. 6).

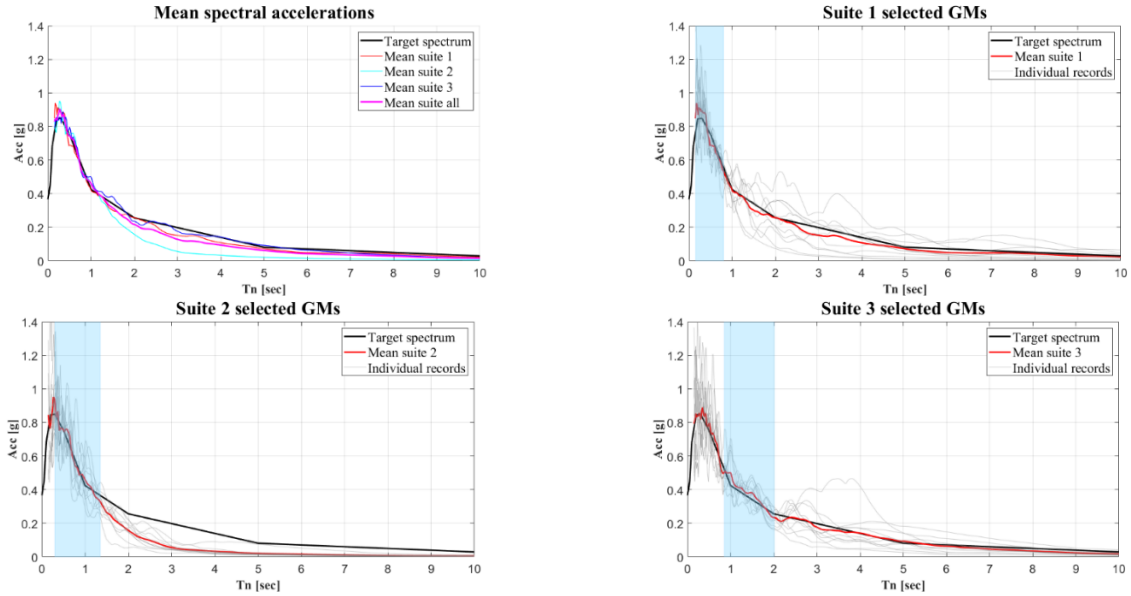

Fig. 6 – Selected/scaled ground motion records.

4.2 Modelling

Given the comparison purpose, two OpenSees models were created for each braced frame (2- and 4-storey). Model A used the classical brace modelling technique (i.e. with no flange local buckling) and Model B

accounted for flange local buckling using the modelling approach described previously. In both models, the brace initial out-of-straightness was set to be 1/1000 of the brace length. This value was selected as it provided excellent match with the test results in model calibration process. Beams and columns were modelled using elastic beam elements with linear geometrical transformation. Beams were modelled as pin- connected to the columns and since gusset plates were modeled as part of the braces, brace nodes were rigidly connected to the columns throughout rigid links. The length of the rigid links was calculated to represent the actual depth of the beams and columns. No P-delta column was included in the model, as the analysis was only to capture the earthquake response component without the effects of gravity loads. Damping was modeled using Raleigh mass/stiffness proportional model considering 3% critical damping in the first two modes of the structure. Stiffness related damping was assigned only to the non-yielding elements based on initial stiffness.

4.3 Response history analysis results

Nonlinear response history analysis was conducted on both frame models (2- and 4-storey) using the previously defined ground motions and considering both brace Models A and B. Peak storey drifts and residual storey drift ratios are presented in Fig. 7 and 8 respectively. In the plots, the thicker black solid lines represent the design seismic demand corresponding to the envelope of the mean demand values determined for each suite of ground motions, as specified in the NBC. For the 2-storey frame, Model B with local buckling demonstrated slightly larger storey drifts when compared with model A, which was expected given the brace section reduction in Model B. However, drifts in both models were within the NBC specified limit of 2.5% times the storey height. Similar slightly larger drifts were also noticed for the 4-storey frame with Model B. For this frame, however, drifts exceeded the NBC limit under 5 ground motions with Model A and 10 ground motions with Model B. Drift exceedance under individual ground motions is not alarming considering the unusual frame configuration in terms of brace sizes, storey heights and seismic weights and that the seismic design values represented by the thick black lines are within the code limit. The main result from this comparison is that flange local buckling in the braces of had very limited consequences on the peak storey drift response of the two structures studied. Similarly, Model B demonstrated for both frames a negligible increase in residual storey drift ratios when compared with Model A (Fig. 8).

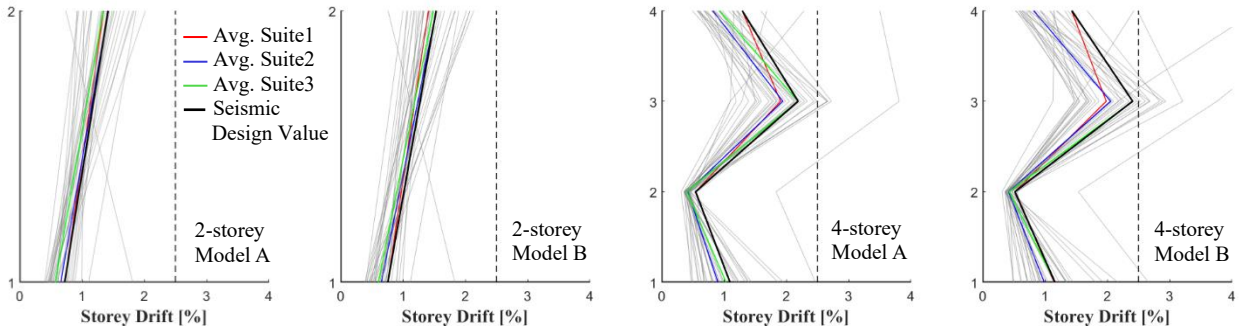

Fig. 7 – Storey drift ratios

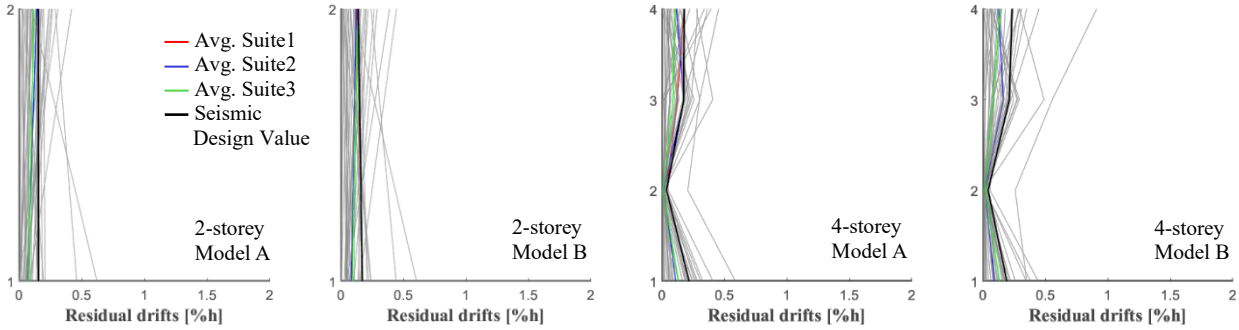

Fig. 8 – Storey residual drift ratios

To further evaluate the effect of brace local buckling on peak storey drifts, the differential drifts between Models A and B are presented in Fig. 9. It is shown that the brace local buckling effects on storey drift is more pronounced for the taller, 4-storey frame. The differential values also generally higher in the upper storeys of the structures.

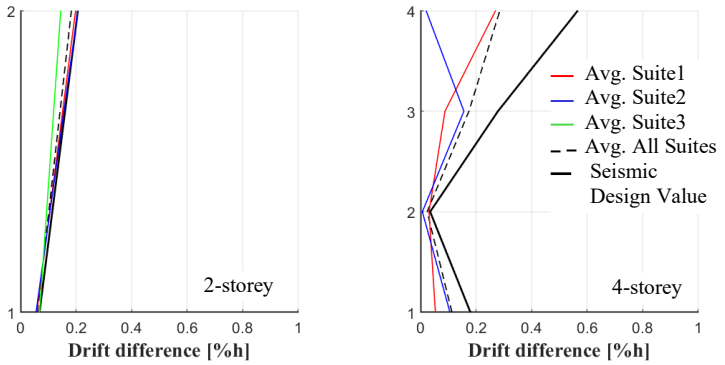

Fig. 9 – Differential storey drifts between Models A and B

To further investigate how brace local buckling can affect the frame storey drift response, the responses of the 4-storey frame is examined under two ground motion cases. Case I is a shallow crustal earthquake ground motion for which differences between the responses from Models A and B are small. Case II is a longer duration interface subduction earthquake ground motion for which Models A and B gave significantly different responses. Storey drift histories and brace force histories in the 3rd storey of the frame are plotted for both cases in Fig. 11 and 12, respectively. For each case, the figures also present the percentages of "buckled" fibers in Model B, i.e. the number of fibers removed out of the possible maximum number governed by the number of elements and the range *R* (Table 1). Values of T_u, C_u and C'_u presented in the brace force histories respectively correspond to the probable yield tensile resistance, probable brace compressive resistance and post-buckling probable resistance of the bracing member, as determined with CSA S16 provisions. The hysteretic responses of the two braces at the 3rd level are also plotted for Cases I and II in Fig. 10.

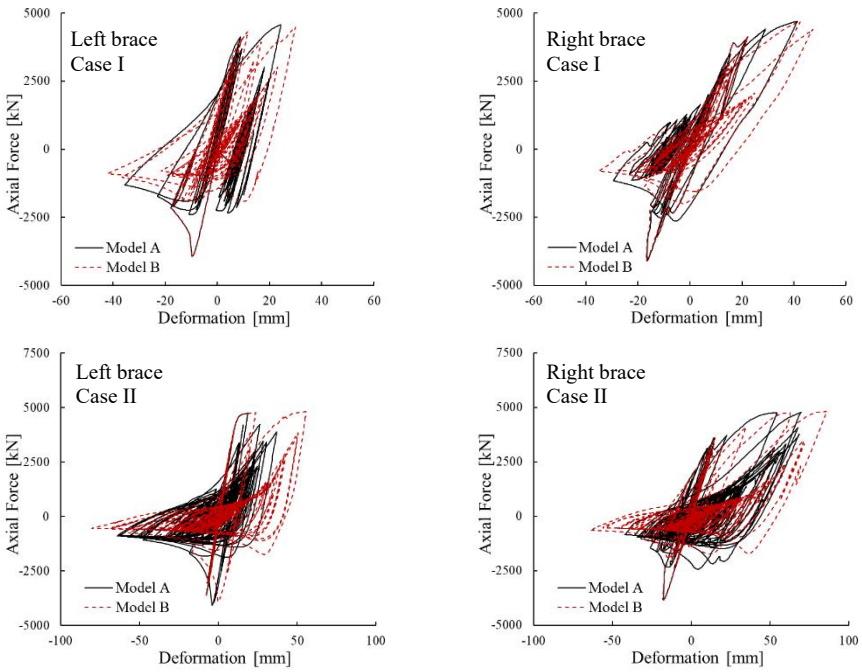

Fig. 10 – Hysteretic responses of the 3rd floor braces of the 4-storey frame

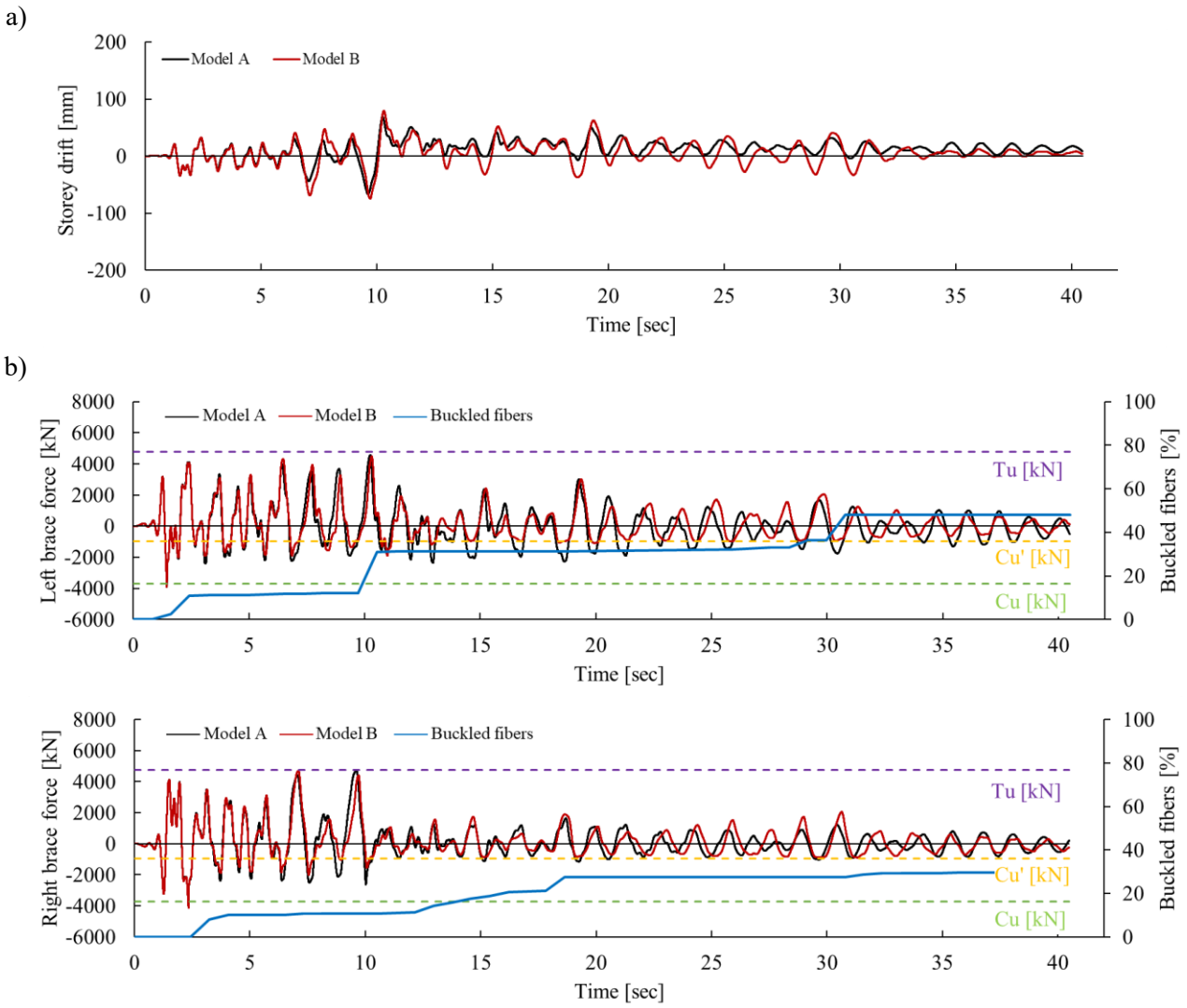

Fig. 11 – Response histories at the 3rd floor of the 4-storey frame for Case I.
a) Storey drifts; b) Brace forces

As expected, both models in both cases predict identical storey drift responses prior to brace local buckling. For Case I in Fig. 11, brace local buckling initiates at approximately 2-3 s, during the occurrence of global buckling of the braces in the first large cycle. Small differences in drifts are then noticed in the subsequent cycles as local buckling affected the moment of inertia of the brace section, reducing the brace compressive strength. As shown, both braces did not reach yielding in tension and this compressive strength reduction did not affect much the storey drifts as the frame drift response was governed by the braces acting in tension.

Conversely, for Case II, the higher percentage of buckled fibers in case II caused a significant difference in peak story drift (Fig. 12a). Examining the brace-force history for case II (Fig. 12b) showed that the reduction of brace axial stiffness due to local buckling also did not lead to a full yielding of the brace acting in tension under the ground motion seismic demands. Similar observation was noticed by plotting the hysteretic response of both braces (Fig. 10), where a perfect match was observed between both brace models within introductory peak cycles. However, with the increase of number of cycles, the effect of stiffness reduction caused larger displacement response in both cases.

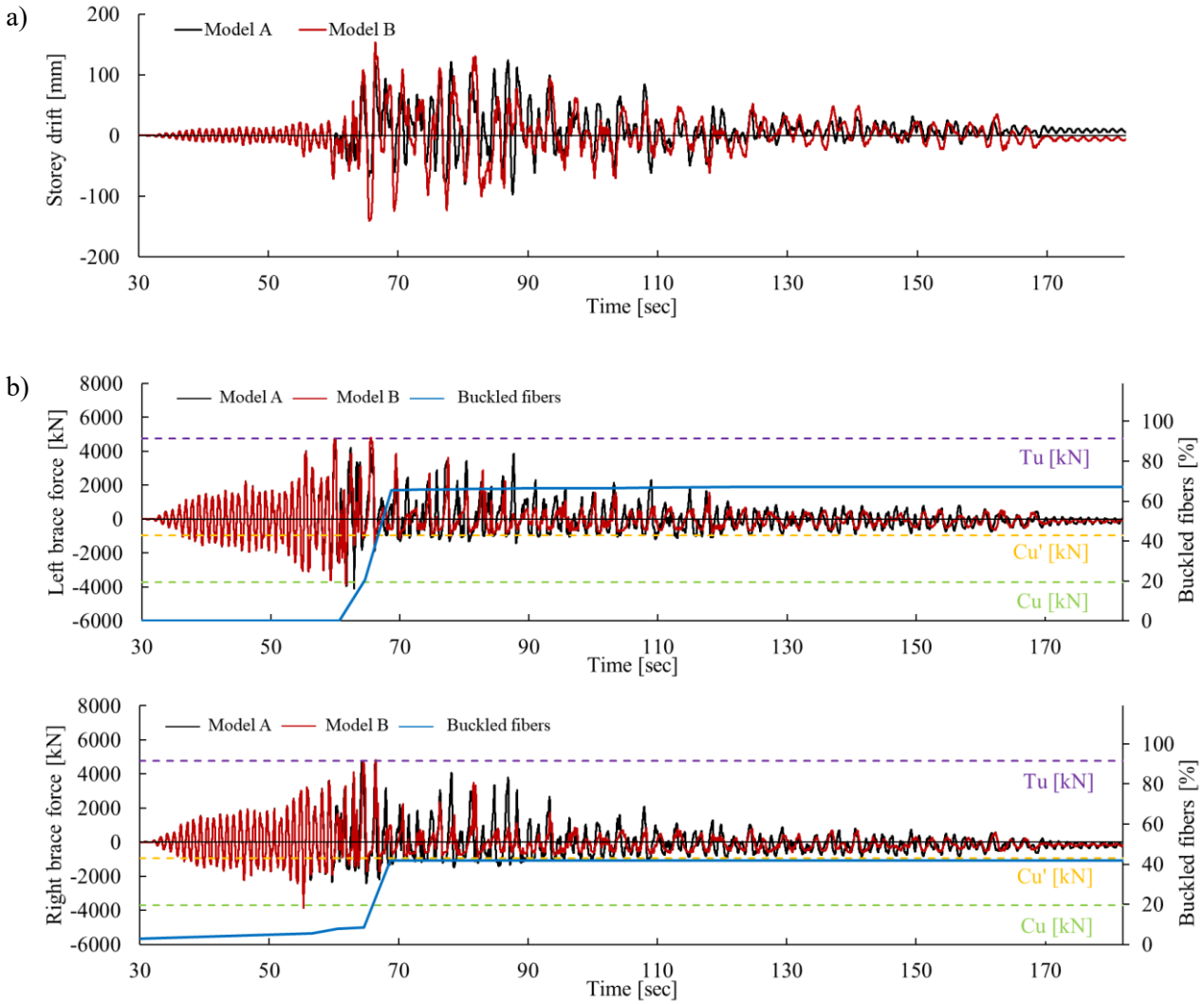

Fig. 12 – Response histories at the 3rd floor of the 4-storey frame for Case II.
a) Storey drifts; b) Brace forces

5. Conclusions

This article presented a study in which an OpenSees modelling technique was developed to account for flange local buckling in I-shaped braces in concentrically braced frames. The technique simulates the reduction in section capacity due to local buckling by cancelling the exterior fibers of the brace flanges during analysis. Additional modelling parameters that allows calibration to be conducted on material and element levels are defined and calibrated using data of full-scale specimens tested previously. The developed modelling technique demonstrated an improved accuracy for predicting the hysteretic response under quasi-static loading when compared with the classical modelling approach.

The paper also evaluated the effect of flange local buckling on the response of 2- and 4-storey braced frames under three types of ground motions (i.e. crustal, in slab, and subduction interface). The frames were designed to accommodate the exact braces tested previously to ensure adequate simulation of local buckling effects. It was shown that although local buckling has a significant effect on the responses at the element level (cyclic test response), its effects on the structural response were limited. The response history analysis showed that,

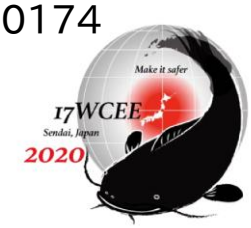

on average, accounting for local buckling slightly increased the average story drifts (< 0.2% h), because storey drifts in the studied structures were mainly controlled by the braces acting in tension.

6. Acknowledgments

Financial support was provided by the Québec Aide financière aux études (AFE) and Natural Sciences and Engineering Research Council of Canada (NSERC). The authors would also like to thank Prof. Mathew Eatherton for his most useful suggestions and comments on the brace model.

7. References

[1] AISC (2016): ANSI/AISC 341-16, *Seismic Provisions for Structural Steel Buildings*, American Institute of Steel Construction (AISC), Chicago, Illinois, USA.

[2] CSA (2014): *CAN/CSA S16-14, Design of Steel Structures*. Canadian Standard Association (CSA), Toronto, Canada.

[3] Astaneh-Asl A, Goel SC, Hanson RD (1986): Earthquake-resistant design of double-angle bracings. *Engineering Journal*, **23**(4), 133-147.

[4] Black RG, Wenger W, Popov EP (1980): Inelastic buckling of steel struts under cyclic load reversals. *Report no. UCB/EERC-80/40*, Earthquake Engineering Research Center, Univ. of California, Berkeley, USA.

[5] Nakashima M,Wakabayashi M (1992): Analysis and design of steel braces and braced frames in building structures. in Stability and Ductility of Steel Structures under Cyclic Loading, Y. Fukumoto and G.C. Lee, editors, CRC Press, Boca Raton, USA 309-321.

[6] Tremblay R, Haddad M, Martinez G, Richard J, Moffatt K (2008): Inelastic cyclic testing of large size steel bracing members. *Proc. 14th World Conference on Earthquake Engineering*, Beijing, China, Paper no. 05-05-0071.

[7] Han SW, Kim WT, Foutch DA (2007): Seismic Behavior of HSS bracing members according to width–thickness ratio under symmetric cyclic Loading. *Journal of Structural Engineering*, **133**(2), 264-273.

[8] Fell B, Kanwinde A, Deierlein, G, Myers, T (2009): Experimental investigation of inelastic cyclic buckling and fracture of steel braces. *Journal of Structural Engineering*, **135**(1), 19-39.

[9] Zeng L, Zhang W, Ding Y (2019): Representative strain-based fatigue and fracture evaluation of I-shaped steel bracing members using the fiber model. *Journal of Constructional Steel Research*, 160, 476–489.

[10] Shim D-Y, Kim H-J (2018): Experimental investigation on inelastic cyclic behaviour of bracing member with wide-flange section. *Proceedings IOP Conf. Series: Materials Science and Engineering,* 371, 012030.

[11] Haddad M (2017): Cyclic behavior and finite element modeling of wide flange steel bracing members. *Thin-Walled Structures,* 111, 65-79.

[12] Haddad M, Shrive N (2019): Investigating the inelastic cyclic behaviour of large-size steel wide-flange section braces. *Construction and Building Materials*, 199, 92-105.

[13] Mazzoni S, McKenna F, Scott MH, Fenves GL (2006): *OpenSees Command Language Manual*. University of California Berkeley: Pacific Earthquake Engineering Research Center, Berkeley, USA.

[14] Aguero A, Izvernari C, Tremblay R (2006): Modelling of the seismic response of concentrically braced steel frames using the OpenSees analysis environment. *Int. J. of Advanced Steel Construction*, **2**(3), 242-274.

[15] Uriz P, Filippou FC, Mahin SA (2008): Model for cyclic inelastic buckling of steel braces. *Journal of Structural Engineering*, **134**(4), 619-628.

[16] Sen A, Roeder CW, Lehman DE, Berman JW (2019): Nonlinear modeling of concentrically braced steel frames. *Journal of Constructional Steel Research*, 157, 103-120.

[17] Hsiao PC, Lehman DE, Roeder CW (2013): A Model to simulate special concentrically braced frames beyond brace fracture. *Earthquake Engineering & Structural Dynamics,* **42**(2), 183-200.

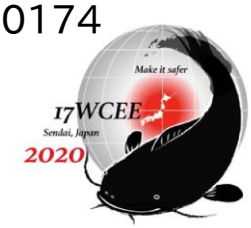

[18] Bosco M, Trica L (2017): Numerical simulation of steel I-shaped beams using a fiber-based damage accumulation model. *Journal of Constructional Steel Research,* 133, 241-255.

[19] Lamarche CP, Tremblay R (2011): Seismically induced cyclic buckling of steel columns including residual-stress and strain-rate effects. *Journal of Constructional Steel Research*, **67**(9),1401-1410.

[20] NRCC (2017): *Structural Commentaries (User's Guide – NBC 2015: Part 4 of Division B)*, 4th ed. National Research Council of Canada (NRCC), Ottawa, Canada.

